ISSN 1392–1320 MATERIALS SCIENCE (MEDŽIAGOTYRA). Vol. 22, No. 3. 2016

Spark Plasma Sintering of Dielectric Ceramics $Zr_{0.8}Sn_{0.2}TiO_4$

Pavel CTIBOR [1]*, Tomáš KUBATÍK [2], Josef SEDLÁČEK [1], Jiří KOTLAN [2]

[1] *Czech Technical University in Prague, Faculty of Electrical Engineering, Department of Electrotechnology, Technická 2, 166 27 Prague 6, Czech Republic*
[2] *Institute of Plasma Physics ASCR,v.v.i., Za Slovankou 3, Prague, Czech Republic*

crossref http://dx.doi.org/10.5755/j01.ms.22.3.8767

Received 24 November 2014; accepted 14 July 2015

Zirconium-tin titanate ceramics (Zr,Sn)TiO_4 was prepared by spark plasma sintering (SPS) technique. Resulting samples, low-height cylinders, were subjected to microstructural observations, immersion measurements of density and porosity and X-ray diffraction phase analysis. Dielectric parameters – relative permittivity and loss factor – were tested in the frequency range from 80 Hz to 1 MHz and volume DC resistivity was measured at 100 volts.
Keywords: titanates, dielectric ceramics, spark plasma sintering.

1. INTRODUCTION

(Zr,Sn)TiO_4, materials were used as dielectric resonators microwave filters and oscillators [1]. An applicability of (Zr,Sn)TiO_4 for humidity sensors is also being investigated [2].

Zirconium-tin titanate (Zr,Sn)TiO_4 belongs to the system $A_{1-x}^{4+}B_x^{4+}Ti^{4+}O_4^{2-}$, in which radii of cations A and B must differ markedly to avoid substitutions in the basic lattice $A^{4+}Ti^{4+}O_4^{2-}$ and subsequent resulting lattice defects affecting dielectric properties. Combination of Zr at the A-position and Sn at the B-position fulfills this requirement. In this work x = 0.2 is used and the material is denoted as ZST. In contrast to the displacive transitions, which take place at discrete temperature, $ZrTiO_4$ exhibits a continuous phase transition of the incommensurate phase to normal phase over the temperature range 1100 to 1200 °C by decreasing lattice order of the Zr-Ti distribution [3]. $ZrTiO_4$ can be used as an additive into ZrO_2 to minimize cracking induced by volumetric changes, when pure ZrO_2 is heated and cooled over transformation temperatures [4].

The $Zr_{0.8}Sn_{0.2}TiO_4$ ceramic materials are typically prepared by a sol-gel technique [1]. In such a process, the pellets are finally sintered in a furnace at 1400 °C for 3 hours holding time at a heating and cooling rate of about 10 °C/min.

Sintering temperatures of dielectric ZST ceramics still remained as high as 1350 °C. The methods including glass additions, wet chemical processing, and liquid-phase sintering aids have been typically used to lower the sintering temperature of ZST ceramics. Using glass additives was found to effectively lower the sintering temperature. Nevertheless, it worsened the dielectric properties of ZST ceramics. The wet chemical processes, especially the co-precipitation route, offered advantages over traditional processing techniques, but often required a complicated procedure that would increase the cost and time in fabricating the ZST ceramics. It is difficult to fully densify ZST ceramics without sintering additives if the powder is prepared by conventional solid-state reaction methods [5, 6]. In contrast, the sintering temperature of ZST ceramics with $BaCuO_2$+CuO, CuO, or V_2O_5 additions could be effectively reduced without decreasing the dielectric properties due to the liquid phase effects. The dielectric properties of ZST ceramics were however strongly sensitive to processing conditions and microstructure features. The relative permittivity was not significantly affected by various additives while the loss factor was strongly dependent on the type and the amount of additives [7].

Spark plasma sintering (SPS) was used in the recent time for processing of dielectric ceramics, although the SPS technique brought a structural disorder [8] that affected also dielectric properties [9]. The SPS process is fast and thanks to it a grain over-growth was successfully blocked in dielectric ceramics [10].

Our paper describes an attempt to lowering of sintering temperature and significant shortening of sintering time of the ZST ceramics (using a powder with the composition $Zr_{0.8}Sn_{0.2}TiO_4$, most interesting composition for the dielectric use [1]) by means of the spark plasma sintering (SPS) technique [11]. The product of this process is subsequently subjected to dielectric characterization with the aim to find the best temperature for SPS fabrication of ZST ceramics.

2. EXPERIMENTAL

2.1. Materials and manufacturing

The material was obtained in the form of broken segments of ceramic pellets produced by reactive sintering using micropowders. Commercially available products from a ceramic dielectric ZST material are known in the Czech Republic under label Stabilit E37. The trade name means that the relative permittivity value $\varepsilon_r = 37$. As-received ceramic segments were crushed and milled into a powder of the size fine enough for SPS processing (size of about 2 μm).

Spark plasma sintering was done using the apparatus SPS 10-4 (Thermal Technology, USA), the process was

* Corresponding author. Tel.: +420 266 053717; fax: + 420 286 586 389.
E-mail address:*ctibor@ipp.cas.cz* (P. Ctibor)

maintained in a "vacuum regime" and with applied specific pressure 80 MPa, dwell time on maximum temperature 4 min. Other parameters were varied for individual samples, as summarized in Table 1. The whole duration of the SPS procedure was only about 25 minutes, contrary to conventional sintering that need minimum 5 hours.

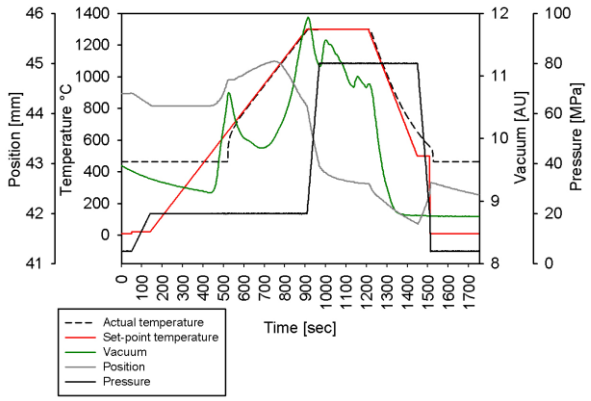

Fig. 1. Main parameters of the SPS processing of the sample C

2.2. Preparation of samples for dielectric measurements

A three-electrode measurement fixture was used to evaluate dielectric parameters of all samples. A thin layer of aluminum was sputtered in a reduced pressure over the sample surface to serve as electrodes. The central circle separated by a gap (produced via surface masking) from the earth electrode covering the rim of the topside surface serves as working electrode. The whole bottom side was covered completely with an Al layer serving as the second working electrode.

2.3. Phase composition

Starting SPS powder and sintered disks (samples) were analyzed by X-ray diffraction. The aim was to obtain crystalline phases identification. All samples were measured in the same manner on Bruker D8 Advance diffractometer in Bragg-Brentano geometry with Cu-Kα radiation and 1D LynxEye detector, precise alignment of the sample surfaces was maintained by a laser.

2.4. Electrical measurements

Capacity was measured in the frequency range from 80 Hz to 1 MHz using programmable LCR-meter (4263B, Agilent, USA). The test signal voltage was 1V AC and the field was applied via the sample fixture Agilent 16451B. Relative permittivity ε_r was calculated from measured capacities and specimen dimensions. The same LCR-meter was used for the loss factor $tg\ \delta$ measurement (at the same frequencies as capacity).

Electric resistance was measured with an adapter Keithley 6105. The electric field was applied from a regulated high-voltage source and the values read by a multi-purpose electrometer (617C, Keithley Instruments, USA). The magnitude of the applied voltage was 100 ± 0.05 V DC and the time of exposure 10 min. Volume resistivity was calculated from the measured resistance and specimen dimensions.

2.5. Atomic force microscopy and light microscopy

The model 7500 (Agilent, USA) Scanning Probe Microscope was used to perform the atomic force microscopy experiments. The system was equipped with a standard 90 µm scanner and a triple-lock in MAC-III controller.

Light micrographs were taken on a polished section perpendicular to the sample surface. The microscope used was Neophot 32 (Zeiss, Germany) at magnification 250x.

Table 1. SPS samples; dwell time for the samples A-C was 4 min

Sample	Temperature, °C	Resistivity, Ωm	ε_r at 1 MHz	$tg\ \delta$ at 1 MHz
A	1100	2.88×10^7	19.7	0.0157
B	1150	1.90×10^7	35.9	0.0397
C	1300	1.42×10^7	40.2	0.0402
B2	sample B annealed at 1000 °C/2 h/air	6.77×10^8	36.2	0.0022
D	1150, dwell time 5 min	1.69×10^8	41.0	0.0760
E	1150, dwell time 5 min, powder X	1.36×10^9	43.2	0.0511
A2	sample A annealed at 1000 °C/8 h/air	8.99×10^{11}	26.8	0.001
Stabilit E37	commercial, furnace-sintered	3.5×10^{12}	37.0	0.001
Note: powder X was the same but crushed to 0.5 – 1 µm				

3. RESULTS AND DISCUSSION

The progress of sintering process is displayed in the Fig. 1. When "vacuum" increases, in fact pressure in the chamber increases. The "actual temperature" inside the SPS cell is after the start displayed correctly after reaching 400 °C, not before. So the first increase in the air pressure (around 400 °C) is the release of moisture from the powder. The second increase in the air pressure (around 900 s; at 1200 °C) corresponds to the time of application of a maximum piston force to press the sample. After, there are some little up and down shifts during sintering. Finally, the air pressure decreases when the sample temperature starts to decrease. In the Table 1 all samples are set into groups according the volume resistivity values. Sample A, sintered at 1100 °C, had the lowest relative permittivity, which is stable versus the varying frequency in the whole range, Fig. 2. Its loss factor is also the lowest and relatively very stable, Fig. 3, with values between 0.1 for low frequency and 0.01 for high frequency. The relative permittivity of the sample A is slightly below the nominal value of the reference material Stabilit E37. When the sintering temperature rose to 1150 °C (for the sample B), both the permittivity and loss factor grew and became frequency dependent, however only in a small extent. When the sample B was after SPS annealed to 1000 °C for 2 hours in air, permittivity as well as loss factor remained very similar to the non-annealed sample. The loss factor is more frequency-dependent for the annealed sample, c.f. B2 in Fig. 3. Further increase of the sintering temperature to 1300 °C, sample C, led to dramatic increase of the permittivity and loss factor at low frequencies, below

300 kHz. Up to 1 kHz, the permittivity of the sample C was higher than 150 and loss factor as high as 0.7. The resistivity of this sample was the lowest, Table 1. Observation done on this set of samples was as follows: The higher the sintering temperature, the lower the resistivity. However, it was always in the order 10^7 Ωm, only for the annealed sample B2 it was 10^8 Ωm.

The sample A was not rigid enough. At machining and polishing of its surface the quantity of debris per a fixed time was markedly larger than for the samples sintered at higher temperatures. With the aim to obtain more rigid sample with enhanced dielectric properties we have modified the manufacturing procedure for the sample B with a longer dwell time, 5 min, to obtain sample D. Its resistivity was considerably higher than for sample B. However, the permittivity was high and very unstable versus changing frequency below 40 kHz. And moreover, the loss factor was below 40 kHz non-acceptably high. This behavior could be joined with due to Maxwell–Wagner type relaxation.

We attempted to other modification of the SPS procedure of the sample B by the longer dwell time, 5 min, and moreover use of a finer powder "powder X", to obtain sample E. Its resistivity was considerably higher than for samples B and D. The permittivity was about 70 at 1 kHz and dropped to about 45 at 1 MHz. The loss factor dropped from 0.25 to 0.05 for the same range.

We should notice that the temperature for sintering ZST dielectric material by SPS (to get similar characteristics as Stabilit E37) is below 1150 °C and may be even below 1100 °C. However, the problems with the bad mechanical quality of such samples are mentioned above. Around 1100 °C, phase transformation, as described in the Introduction, took probably place. Annealing for only 2 hours in air did not improve significantly the properties. Longer dwell time at SPS, however, worsened the dielectric behavior remarkably. Depending on the sample processing route of ZST, relatively large variety of relative permittivity values from 30 to 60 was reported by other authors [12]. The high value of the permittivity at a low frequency region is attributed to space charge polarization due to charged lattice defects [1**,** 12]. Similarly to authors studying a sol-gel prepared ZST [1], we obtained at room temperature resistivities in order of 10^7 Ωm and relative permittivity stable for our best samples at the whole frequency range. The explanation of the polarizing mechanisms provided in [1] seems to be plausible also for our samples.

In the next step we have modified the procedure for manufacturing of sample A by a long duration thermal post-treatment to obtain sample A2. Its resistivity was considerably higher than for sample A and reached nearly the value of the reference sample - commercial Stabilit E37, Table 1. The permittivity was about 26.85 at 1 kHz and raised slightly, to about 28.80 at 1 MHz – in other words, it was very stable. The loss factor dropped from 0.005 to 0.001 for the same range.

However, interesting is that both these improved-resistivity samples, E and A2, were porous, c.f. Table 2. The extremely high porosity of the sample A was not eliminated by the thermal post-treatment. Similarly, the high porosity of the sample B was not suppressed by SPS process modifications leading to obtaining the sample E.

Table 2. Density and open porosity determined by the water immersion technique

Sample	SPS temperature, °C	Density, $g \cdot cm^{-3}$	Open porosity, %
A	1100	3.8923	24.6
B	1150	4.4273	14.3
C	1300	5.0178	0.3
B2	sample B, annealed at 1000 °C/2 h/air	4.5767	10.5
D	1150 (dwell time 5 min)	n.a.	n.a.
E	1150 (dwell time 5 min) powder X	4.4846	13.2
A2	sample A, annealed at 1000 °C/8 h/air	3.9322	22.6

The high density of sample C did not imply its high electrical resistivity. Its high manufacturing temperature is associated with reduction of oxygen in the titanate site.

X-ray diffraction revealed presence of Srilankite phase (PDF card 01-080-1783), which is either $ZrTiO_4$ or $(Zr,Sn)TiO_4$. All the samples exhibited the same character of the XRD pattern.

We can confirm the statement [2] that ZST samples do not start to lose their high porosity until sintering temperatures higher than 1300 °C. Our samples exhibit approximately the same trend and also temperature frames for relative permittivity as in the publication [7], where the authors used V_2O_5 as an agent promoting the conventional sintering. The dispersion of porosity values is huge among our samples and therefore the mechanisms responsible for the dielectric behavior would vary sample to sample, including the influence of adsorbed water in pores for the high porosity samples.

Samples C and D could be considered according the Fig. 2 and Fig. 3 as having a broad peak on both the permittivity and the loss characteristics, which peak has a maximum at low frequencies, outside the measured range [13]. For the Maxwell–Wagner (M-W) type relaxation an additional capacitance comes from extrinsic sources such as grain/grain-boundary charge accumulation. When a current flows across the interface, charges are accumulated at the interface [14]. Elsewhere is it mentioned as an internal barrier layer [15]. The grain interior contribution to the polarization manifests itself mainly as a high-frequency component whereas the grain-boundary component takes place at low frequency, where it increases the relative permittivity as well as the losses [13]. In our case, mainly samples C and D exhibit M-W relexation, but also other samples are influenced by the grain boundaries.

Atomic force microscopy was done in topographical (tapping) mode as well as in electric potential mode for the area 3 x 3 μm, Fig. 4. The 3D topographical image of the sample B shows many grains, whereas its total height variation is 1.7 μm. The surface was quite rough for typical AFM investigations.

The topographical image overlaid with the surface potential mapping image revealed higher potential at some

grain edges (~ 150 mV higher than the surface main value) as well as lower potential (blue) in some spots of ~ 100 mV.

Fig. 5 shows the microstructure of the sample B in a cross section. The particles are typically 2 – 3 μm large, but there exist granular or elongated particles with at least one dimension substantially larger, up to 10 μm. Such particles exhibit internal globular porosity. The degree of sintering is not very high and the structure exhibits high porosity level.

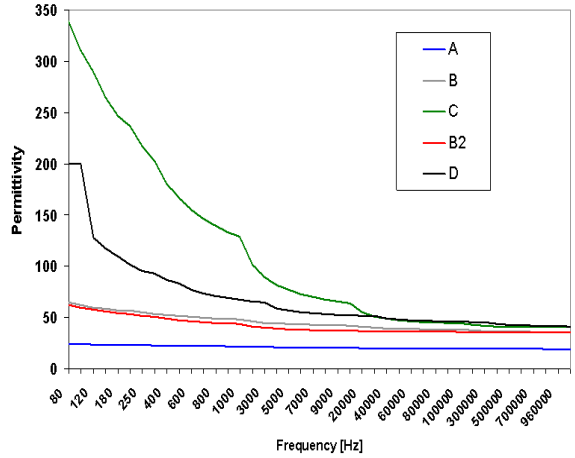

Fig. 2. Relative permittivity of the SPS samples

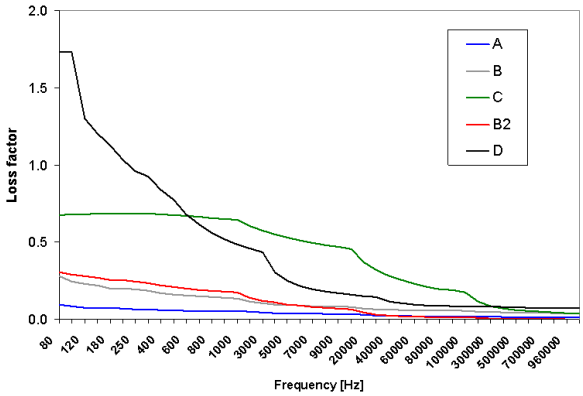

Fig. 3. Loss factor of the SPS samples

The samples B and B2 were tested in microwave frequency range using a strip resonator. In this case the geometrical compliance of the sample to the electric field is not optimal, but the estimation of resonance frequency using an oscilloscope can provide informative values. The sample B2 had the resonance frequency at 2.02 GHz whereas the sample B did not resonate until 3 GHz when the frequency was continuously tuned up. The thermal post-treatment of SPS samples lead typically to a grain growth [16]. The lower resonance frequency for the annealed sample B2 is a sign of its coarser grains [17].

Finally, we can conclude that the phase transformation around 1100 °C complicates markedly the processing of ZST dielectric ceramics also for a pressure-assisted process such as SPS. If ZST is densified without sintering additives, the obtaining of samples with a mechanical rigidity comparable with the bulk reference material and in the same time with good dielectric response in the radio frequency region is not able. The only way is to sinter samples at SPS just under the transformation temperature and anneal it subsequently even deeper below the transformation temperature, but for long time. However, via this two-step process the initial advantage of the fast SPS procedure is not applicable.

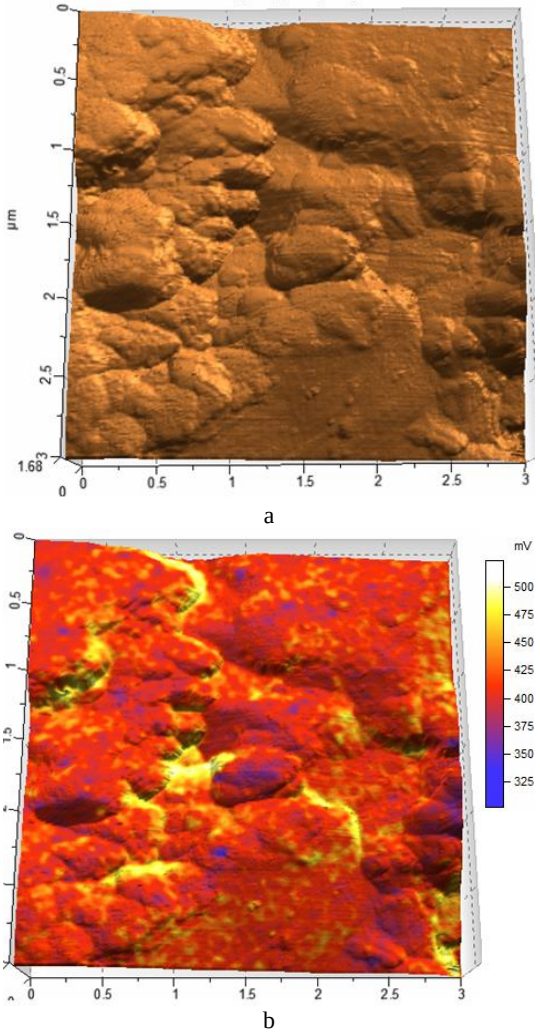

Fig. 4. a – AFM image of the surface, topographic mode, b – topographic mode (relief) overlaid with potential mode (colors)

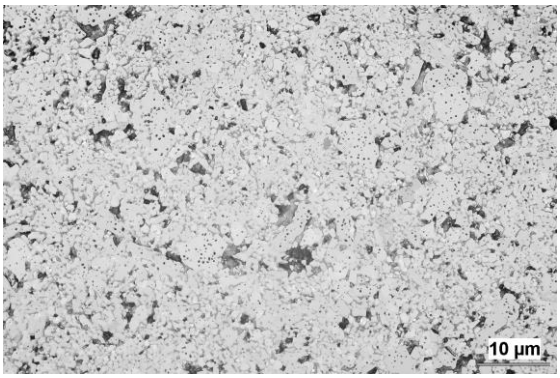

Fig. 5. Microstructure of SPS, sample B; optical micrograph of a cross section

4. CONCLUSIONS

Zirconium-tin titanate ceramics $(Zr,Sn)TiO_4$ was prepared by a spark plasma sintering (SPS) technique. The higher the sintering temperature was, the lower was the electric volume resistivity – but it was always in the order

10^7 Ωm, only for the sample annealed for 2 hours it was 10^8 Ωm. If the dwell time on the maximum temperature at SPS rose, the resistivity was in order 10^8 Ωm, and when considerably finer powder was used with such prolonged dwell time, it rose to 10^9 Ωm. Only when subsequent annealing was applied and its time increased to 8 hours, the resistivity increased to 10^{11} Ωm that is approaching the resistivity of the conventionally sintered reference sample.

The whole duration of the SPS procedure was only about 25 minutes, but for obtaining acceptable dielectric responses, subsequent thermal post-treatment for as long as 8 hours was necessary. Via this two-step process the initial advantage of the fast SPS procedure is not applicable. Further investigation focused on relations between the powder size and processing parameters would bring further progress in optimization of ZST manufactured by SPS.

Acknowledgment

The authors thank to G. Kada for the AFM measurements, to V. Papež for strip resonator to K. Neufuss for immersion porosimetry, and Z. Pala for XRD phase analysis. The work was supported by the Czech technical university grant SGS13/195/OHK3/3T/13.

REFERENCES

1. **Ganesh, Babu, P., Kumar, C., Ravichandran, K., Manohar, P.,** Synthesis and Characterization of Zirconium Tin Titanate ($Zr_{0.8}Sn_{0.2}TiO_4$) *International Journal of ChemTech Research* 5 (5) 2013: pp. 2122 – 2129.
2. **Macan, J., Gajovic, A., Ivankovic, H.** Porous Zirconium Titanate Ceramics Synthesized by Sol–gel Process *Journal of the European Ceramic Society* 29 2009: pp. 691 – 696.
3. **Park, Y., Kim, H. G.,** Effect of Electric Field on the Phase Transition in $ZrTiO_4$ *Journal of Mataterals Science Letters* 16 1997: pp. 1130 – 1132.
4. **Lopez-Lopez, E., Moreno, R., Baudin, C.** Fracture Strength and Fracture Toughness of Zirconium Titanate–Zirconia Bulk Composite Materials *Journal of the European Ceramic Society* 35 2015: pp. 277 – 283. http://dx.doi.org/10.1016/j.jeurceramsoc.2014.08.005
5. **Wakino, K., Minai, K., Tamura, H.** Microwawe Characteristics of (Zr,Sn)TiO_4 and BaO-PbO-Nd_2O_3-TiO_2 Dielectric Resonator *Journal of the American Ceramic Society* 67 (4) 1984: pp. 278 – 281. http://dx.doi.org/10.1111/j.1151-2916.1984.tb18847.x
6. **Iddles, D. M., Bell, A. J., Moulson, A. J.** Relationships Between Dopants, Microstructure and Dielectric Properties of ZrO_2-TiO_2-SnO_2 Ceramics *Journal of Materials Science* 27 1992: pp. 6303 – 6310. http://dx.doi.org/10.1007/BF00576276
7. **Huang, G., Zhou, D., Xu, J., Chen, X., Zhang, D., Lu, W., Li, B.** Low-temperature Sintering and Microwave Dielectric Properties of (Zr,Sn)TiO_4 Ceramics *Materials Science and Engineering B* 99 2003: pp. 416 – 420. http://dx.doi.org/10.1016/S0921-5107(02)00452-X
8. **Su, B., He, J. Y., Cheng, B. L., Button, T. W., Liu, J., Shen, Z., Nygren, M.** Dielectric Properties of Spark Plasma Sintered (SPS) Barium Strontium Titanate (BST) Ceramics *Integrated Ferroelectrics: An International Journal* 61 (1) 2004: pp. 74 – 81. http://dx.doi.org/10.1080/10584580490459017
9. **Ctibor, P., Kubatík, T., Chráska, P.** Spark Plasma Sintering of Multilayer Ceramics – Case Study of Al_2O_3 – Mg(Ca)TiO_3 Sandwich *Key Engineering Materials* 606 2014: pp. 205 – 208. http://dx.doi.org/10.4028/www.scientific.net/KEM.606.205
10. **Herrera, Robles, J. O., Rodriguez, Gonzalez, C. A., Diaz de la Torre, S., Fuentes, Cobas, L. E., Garcia Casillas, P. E., Camacho, Montes, H.,** Dielectric Properties of Bismuth Titanate Densified by Spark Plasma Sintering and Pressureless Sintering *Journal of Alloys and Compound* 536S 2012: pp. S511 – S515.
11. **Eriksson, M.** Spark Plasma Sintering Enhancing Grain Sliding, Deformation and Grain Size Control, *Doctoral Thesis* 2010, Department of Materials and Environmental Chemistry, Stockholm University, Stockholm, Sweden.
12. **Xiong, Z. X., Huang, J. R., Fang, C., Pan, Z. Y.** Hydrothermal Synthesis of (Zr,Sn)TiO_4 Nano-powders for Microwave Ceramics *Journal of the European ceramic society* 23 2003: pp. 2515 – 2518.
13. **Victor, P., Bhattacharyya, S., Krupanidhi, S. B.** Dielectric Relaxation in Laser Ablated Polycrystalline $ZrTiO_4$ Thin Films *Journal of Applied Physics* 94 (8) 2003: pp. 5135 – 5142. http://dx.doi.org/10.1063/1.1606509
14. **Iwamoto, M.** Encyclopedia of Nanotechnology, 2012, Springer, pp. 1276 – 1285.
15. **Chung, U.-C., Elissalde, C., Mornet, S., Maglione, M.** Controlling Internal Barrier in Low Loss $BaTiO_3$ Supercapacitors *Applied Physics Letters* 94 (7) 2009: 072903 – 072911. http://dx.doi.org/10.1063/1.3076125
16. **Zhen, Y., Li, J.-F., Wang, K., Yan, Y., Yu, L.** Spark Plasma Sintering of Li/Ta-modified (K,Na)NbO_3 Lead-free Piezoelectric Ceramics: Post-annealing Temperature Effect on Phase Structure, Electrical Properties and Grain Growth Behavior *Materials Science and Engineering B* 176 2011: pp. 1110 – 1114.
17. **Porokhonskyy, V., Jin, L., Damjanovic, D.** Separation of Piezoelectric Grain Resonance and Domain Wall Dispersion in Pb(Zr,Ti)O_3 Ceramics *Aplied Physics Letters* 94 2009: pp. 212906 – 201914.